Louisiana Transportation Research Center

Technical Assistance Report 19-03TA-P

Structural Assessment of Inundated Roads in Livingston Parish, Louisiana with the Falling Weight Deflectometer

by

Kevin Gaspard, P.E.
Zhongjie Zhang, Ph.D., P.E.
Mark Martinez, P.E.

LTRC

4101 Gourrier Avenue | Baton Rouge, Louisiana 70808
(225) 767-9131 | (225) 767-9108 fax | www.ltrc.lsu.edu

TECHNICAL REPORT STANDARD PAGE

1. Report No.	2. Government Accession No.	3. Recipient's Catalog No.
LTRC 19-03TA-P		

4. Title and Subtitle	5. Report Date
Structural Assessment of Inundated Roadways in Livingston Parish, Louisiana with the Falling Weight Deflectometer	January 2020
	6. Performing Organization Code
7. Author(s)	8. Performing Organization Report No.
Kevin Gaspard, Zhongjie Zhang, and Mark Martinez	19-03TA-P
9. Performing Organization Name and Address	10. Work Unit No.
	11. Contract or Grant No.
12. Sponsoring Agency Name and Address	13. Type of Report and Period Covered
Louisiana Department of Transportation and Development P.O. Box 94245 Baton Rouge, LA 70804-9245	**Technical Assistance Report** **August 2016 to May 2019**
	14. Sponsoring Agency Code

15. Supplementary Notes

Conducted in Cooperation with the U.S. Department of Transportation, Federal Highway Administration

16. Abstract

Researchers discovered strong evidence of damage to Livingston Parish's inundated roadway system during the flood of August 2016. LTRC conducted a comprehensive structural assessment of inundated roadways in Livingston Parish, Louisiana with the falling weight deflectometer (FWD). Treated (inundated) versus non-treated (non-inundated) statistical methods were employed to prove damage. Three parameters from the FWD were used in the analysis, in-place structural number (SN_{eff}), deflection at the first sensor of the FWD (D1), and subgrade resilient modulus (M_r). The damage was translated into an equivalent thickness of asphaltic concrete (AC) pavement from the parameter of SN_{eff} using pavement design methods typically used by the Louisiana Department of Transportation and Development (DOTD).

The data were sorted into three groups based on the thickness of the AC pavement: All data points (all thickness groups), 4 in. to 3 in. group, and 2 in. to 2.5 in. group. The statistical analysis of the entire set of data indicated that statistical differences existed for all three parameters, SN_{eff}, D1, and subgrade M_r. Regarding SN_{eff}, the difference between the mean values of the non-inundated and inundated roadways was equivalent to approximately 1 in. of AC. The differences in the mean values for D1 and subgrade M_r indicated that the inundated pavements were approximately 22.5 percent and 10.3 percent, respectively, weaker than the non-inundated pavements.

Statistical comparisons on the 4 in. to 3 in. thickness group indicated that statistical differences existed for all three parameters, SN_{eff}, D1, and subgrade M_r as with the all thickness group. In the case, the differences in SN_{eff} was equivalent to approximately 2.5 in. of AC. Regarding the D1 and subgrade M_r parameters, the results indicated that the inundated pavements were approximately 56.5 percent and 25.3 percent, respectively, weaker than the non-inundated pavements.

Statistical differences in the three parameters, SN_{eff}, D1, and subgrade M_r for the 2.0 in. to 2.5 in. thickness group were not discovered; however, differences in magnitudes of the means for each parameter were discovered, all indicating that the inundated pavements were weaker than the non-inundated pavements. Regarding the SN_{eff}, the difference in the mean values between the non-inundated and inundated pavements were equivalent to approximately 0.5 in. of AC. The difference in stiffness between the inundated and non-inundated pavements based on the D1 parameter was approximately 22.6 percent, while the strength difference in subgrade M_r was approximately 4.6 percent.

17. Key Words	18. Distribution Statement
Inundation, structural damage, resilient modulus, asphalt pavement, local roads, flood mitigation	**Unrestricted. This document is available through the National Technical Information Service, Springfield, VA 21161.**

19. Security Classif. (of this report)	20. Security Classif. (of this page)	21. No. of Pages	22. Price

Structural Assessment of Inundated Roads in Livingston Parish, Louisiana with the Falling Weight Deflectometer

by

Kevin Gaspard, P.E.
Zhongjie Zhang, Ph.D., P.E.
Mark Martinez, P.E.

Louisiana Transportation Research Center
4101 Gourrier Ave.
Baton Rouge, LA 70808

Technical Assistance Report Number: 19-03TA-P

conducted for

Louisiana Department of Transportation and Development
Louisiana Transportation Research Center

January 2020

ABSTRACT

Researchers discovered strong evidence of damage to Livingston Parish's inundated roadway system during the flood of August 2016. LTRC conducted a comprehensive structural assessment of inundated roadways in Livingston Parish, Louisiana with the falling weight deflectometer (FWD). Treated (inundated) versus non-treated (non-inundated) statistical methods were employed to prove damage. Three parameters from the FWD were used in the analysis, in-place structural number (SN_{eff}), deflection at the first sensor of the FWD (D1), and subgrade resilient modulus (M_r). The damage was translated into an equivalent thickness of asphaltic concrete (AC) pavement from the parameter of SN_{eff} using pavement design methods typically used by the Louisiana Department of Transportation and Development (DOTD).

The data were sorted into three groups based on the thickness of the AC pavement: All data points (all thickness groups), 4 in. to 3 in. group, and 2 in. to 2.5 in. group. The statistical analysis of the entire set of data indicated that statistical differences existed for all three parameters, SN_{eff}, D1, and subgrade M_r. Regarding SN_{eff}, the difference between the mean values of the non-inundated and inundated roadways was equivalent to approximately 1 in. of AC. The differences in the mean values for D1 and subgrade M_r indicated that the inundated pavements were approximately 22.5 percent and 10.3 percent, respectively, weaker than the non-inundated pavements.

Statistical comparisons on the 4 in. to 3 in. thickness group indicated that statistical differences existed for all three parameters, SN_{eff}, D1, and subgrade M_r as with the all thickness group. In the case, the differences in SN_{eff} was equivalent to approximately 2.5 in. of AC. Regarding the D1 and subgrade M_r parameters, the results indicated that the inundated pavements were approximately 56.5 percent and 25.3 percent, respectively, weaker than the non-inundated pavements.

Statistical differences in the three parameters, SN_{eff}, D1, and subgrade M_r for the 2.0 in. to 2.5 in. thickness group were not discovered; however, differences in magnitudes of the means for each parameter were discovered, all indicating that the inundated pavements were weaker than the non-inundated pavements. Regarding the SN_{eff}, the difference in the mean values between the non-inundated and inundated pavements were equivalent to approximately 0.5 in. of AC. The difference in stiffness between the inundated and non-inundated pavements based on the D1 parameter was approximately 22.6 percent, while the strength difference in subgrade M_r was approximately 4.6 percent.

ACKNOWLEDGMENTS

The authors wish to acknowledge the efforts of LTRC's Pavement Unit, Mitch Terrell, Terrell Gorham, and Benjamin Key. Eddie Adyell and Erin Broussard also provided valuable information on Livingston Parish's roadway network and available flood map information from FEMA. Davis "Pepper" Allgood contributed by networking between the various groups and providing valuable information from various FEMA appeals.

TABLE OF CONTENTS

LIST OF TABLES

LIST OF FIGURES

INTRODUCTION

According to the National Oceanic and Atmospheric Administration (NOAA), there have been 233 weather and climatic disasters exceeding $1 billion per event in the United States (US) between 1980 and 2018 *[1]*. It is estimated that the total costs of these events exceeds $1.5 trillion dollars *[1-2]*. As of April 30, 2018, the Federal Emergency Management Administration (FEMA) has reported that there have been 118 significant flooding events since 1978 in the USA, costing over $57 billion *[3]*. Eleven (9.3 percent) of these significant flooding events have occurred in Louisiana *[3]*.

In articles and reports written by several sources, it was estimated that approximately 109,000 homes in Louisiana were inundated during the storm that occurred between August 11 – 13, 2016, hereafter referred to as the August 2016 flood, as presented in Figures 1 to 3 *[4-6]*. The damage caused by the inundation was estimated to be $20 billion *[4]*. The hardest hit parishes were East Baton Rouge and Livingston. In East Baton Rouge Parish, approximately 41,000 homes were flooded while in Livingston Parish 38,000 or 74 percent of the homes were flooded. There were also an estimated 90,000 vehicles flooded and agricultural losses were estimated to be over $110 million dollars. Additionally, approximately 19,900 (20 percent) of businesses were disrupted. This translates into 278,500 workers or 14 percent of the workforce. There is a plethora of publications providing predictions of continual extreme weather events that will ultimately lead to more severe flooding or inundation events *[7-8]*.

Figure 1
Rainfall map from August 11 – 13, 2016

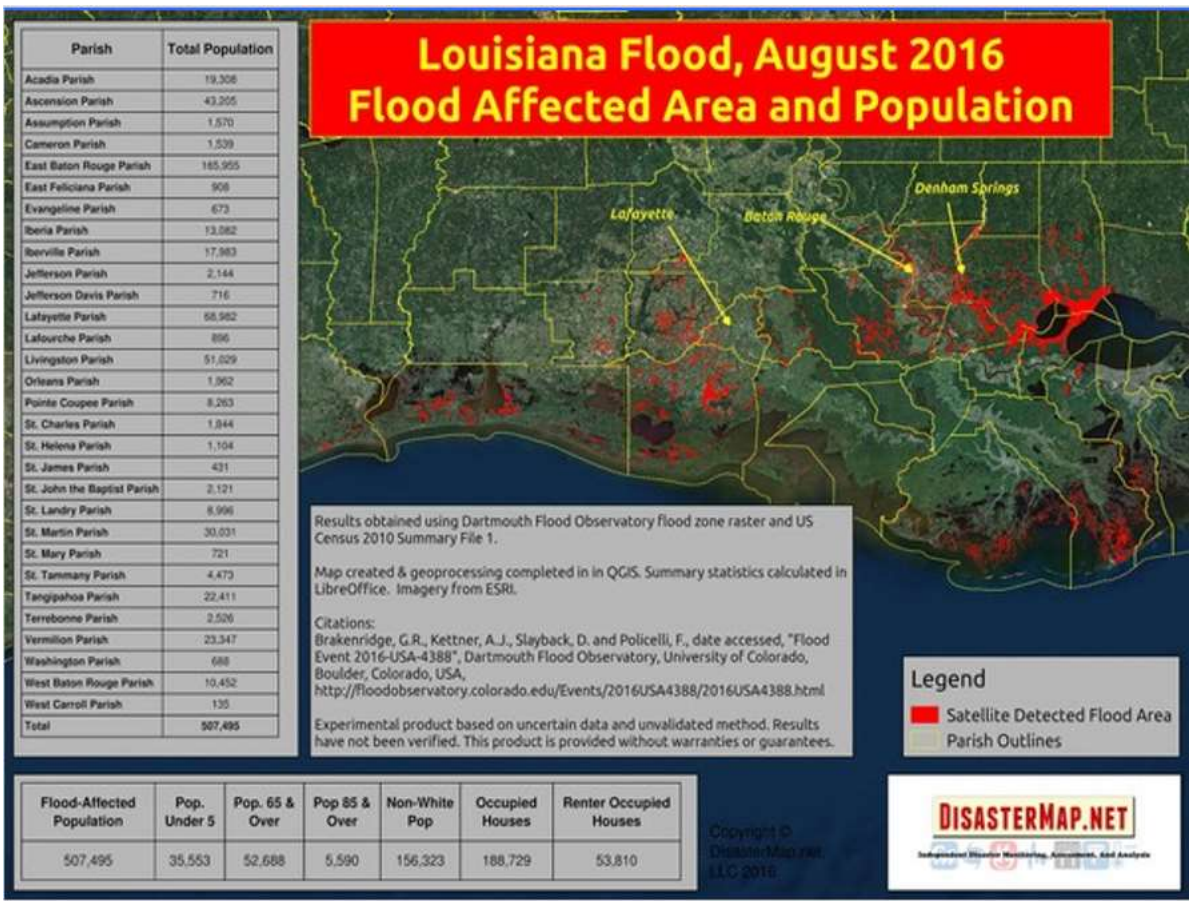

Parish	Total Population
Acadia Parish	19,308
Ascension Parish	43,205
Assumption Parish	1,570
Cameron Parish	1,539
East Baton Rouge Parish	165,955
East Feliciana Parish	908
Evangeline Parish	673
Iberia Parish	13,082
Iberville Parish	17,983
Jefferson Parish	2,144
Jefferson Davis Parish	716
Lafayette Parish	58,982
Lafourche Parish	896
Livingston Parish	51,029
Orleans Parish	1,962
Pointe Coupee Parish	8,263
St. Charles Parish	1,844
St. Helena Parish	1,104
St. James Parish	431
St. John the Baptist Parish	2,121
St. Landry Parish	8,996
St. Martin Parish	30,031
St. Mary Parish	721
St. Tammany Parish	4,473
Tangipahoa Parish	22,411
Terrebonne Parish	2,526
Vermilion Parish	23,347
Washington Parish	688
West Baton Rouge Parish	10,452
West Carroll Parish	135
Total	507,495

Flood-Affected Population	Pop. Under 5	Pop. 65 & Over	Pop 85 & Over	Non-White Pop	Occupied Houses	Renter Occupied Houses
507,495	35,553	52,688	5,590	156,323	188,729	53,810

Figure 2
Population affected by inundation

Figure 3
Parishes in Louisiana with disaster declarations

According to Livingston Parish officials, approximately 400 miles of roads were inundated during the August 2016 flood. LTRC conducted an assessment of 40 miles of the inundated

roads using the falling weight deflectometer (FWD) listed in Appendix A. LTRC's statistical experimental design was based upon testing roadways that were inundated during the August 2016 storm as well as testing roadways that were not inundated. The analysis of variance (ANOVA) method was used to compare the two groups.

Literature Review

Assessments of Inundated Pavement Structures

LTRC has conducted a research study on LA 493 (Natchitoches Parish, Louisiana) that provides strong evidence of damage to roadways caused by inundation *[9]*. The evidence supporting this comes from three sources: a rod and level cross-section survey taken approximately one month prior to the first inundation event and subsequent cross-section surveys taken after the first to third inundation events, from pavement assessments with LTRC's profiler in June 2017 and June 2018, from a structural assessment with the FWD.

Differential movements of the roadway surface were measured after the inundation events. The elevation increase at the centerline of the test sites varied from 0.0961 in. to 1.752 in. after the first inundation event. Movements such as those measured will adversely affect the pavements performance leading to a reduced service life.

Results from the International Roughness Index (IRI) testing implied that (1) there were high degrees of differential profile changes in the roadway surface; (2) the IRI was significantly higher than it should have been for a roadway with its service age; and (3) there was a high degree of IRI variation amongst the test sites. Data from rutting tests also had high degrees of variability. The maximum measured rut depth was 1.685 in.

Longitudinal crack data implied that (1) most of the sites had excessive longitudinal cracking for the time that they were in service; (2) the longitudinal cracking observed is consistent with volumetric changes occurring in the subgrade; and (3) it is logical to infer that the inundation events were responsible for both the magnitude and premature emergence of these longitudinal cracks.

Data from the FWD testing implied that structural damage was present. The amount of damage present ranged from 0.2 to 2.61 in. of equivalent asphaltic concrete thickness.

On August 29, 2005, Hurricane Katrina devastated New Orleans and southeastern Louisiana, leaving hundreds of thousands either displaced or homeless. Nearly four weeks later,

Hurricane Rita made landfall in the southwestern portion of the state, further damaging Louisiana's infrastructure and impacting the New Orleans area once again *[10-11]*.

LTRC conducted a research project to assess the damage caused to DOTD roadways in Orleans, St. Bernard, and Jefferson parishes *[10-11]*. Approximately 235 miles of roadways [asphaltic concrete (AC), composite, and Portland cement concrete (PCC)] were tested with the falling weight deflectometer (FWD), ground penetrating radar (GPR), and dynamic cone penetrometer (DCP). Coring of the roadway was also performed to validate GPR readings as well as determine the type and thickness of the pavement and base course. The soil type was determined using visual inspection from the cores. A typical forensic approach of comparing "before and after" flooding structural conditions could not be conducted on the tested roadways with the exception of one roadway, LA 46 (St. Bernard Parish, Louisiana). Prior to the flood, LTRC had conducted a forensic analysis on LA 46. Comparing the strength of LA 46 before and after the flooding indicated that the damage to its structure was equivalent to approximately 3 in. of AC *[10]*.

In order to conduct a statistical analysis, the pavements were stratified according their type (AC, composite, and PCC) and flooding condition (flooded, non-flooded). From there, they were further stratified based upon depth of inundation, duration of inundation, and pavement thickness. Though there was some variance in the structural damage amongst the groups, all groups generally produced results that confirmed the non-flooded pavements were stronger that the flooded pavements.

Depending upon the data groups, the amount of AC required to mitigate damages to the AC pavements ranged from 0.59 to 3.57 in., composite pavements ranged from 0 to 3.27 in., and PCC pavements ranged from 0 to 1.18 in. It should be noted that these results were based upon a network analysis, and some roadways may actually need more AC to mitigate the damages. This could only be determined by a project-based analysis, which was beyond the scope of this study. Furthermore, the amount of asphalt (3 in.) determined from the "before-and-after" analysis for LA 46 falls within the range for composite pavements (0 to 3.27 in.) as determined by the spatial analysis *[10-11]*.

Stantec Consultant Services conducted a study in 2015, which was not published, for the City of New Orleans entitled, "Quantification of Flood Damage from Hurricane Katrina on the City of New Orleans Pavement Network." There were 310 miles of roadways (20 percent of their network) selected using statistical sampling for assessment with the FWD, GPR, profiler-imaging vehicle, and coring. The streets were stratified into four groups: network

level, neighborhood level, street level, and roadway level. Four major parameters were assigned to the streets in each of the groups previously listed: flood condition, pavement type, subgrade type, and functional class.

The variables used to catalogue the pavement conditions were IRI, pavement quality index, surface distresses, subgrade resilient modulus (M_r), modulus of subgrade reaction (k), in-place structural number (SN_{eff}), and effective slab thickness (D_{eff}). Stantec used a weighted approach to demonstrate the damage caused by the flooding and debris hauling. For AC and composite pavements, they concluded that the damage was equivalent to 1.21 SN or 2.9 in. AC; whereas, the damage to PCC roads was equivalent 0.51 in. D_{eff} or 0.51 in. PCC.

Helali et al. conducted a study for Jefferson Parish in Louisiana *[12]*. Twenty percent (338 miles) of roadways in their network were selected for assessment using statistical sampling methods. The parameters used in their analysis were flooding condition (flooded versus non-flooded), traffic levels, subgrade soil type, jurisdiction, and availability of historical data. Distress data was collected with their Profiler-Imaging vehicle and FWD.

The results of their network level analysis concluded that the flooded pavements were in significantly worse condition than the non-flooded pavements. For AC pavements, the difference in strengths were on average equivalent to 1 SN or 2.3 in. AC. Regarding PCC, the average difference D_{eff} was 0.92, which is equivalent to 0.92 in. PCC.

Vennapusa et al. conducted a study to capture the damage caused by flooding from the Missouri River in Iowa *[13]*. The estimated damage was $63 million to primary and secondary roadways in the counties studied. Roadway testing was conducted with the FWD, DCP, GPR, 3-D laser scanning, and hand auger borings. Assessments were conducted on roadways with gravel, AC, chip sealed, and PCC surfaces.

On gravel roads, results from FWD testing indicated that the flooded gravel roads were significantly weaker than the non-flooded roads based upon the statistical analysis *[13]*. The results also indicated that the subgrade had an 86 percent influence on the FWD measurements, while the gravel had approximately a 14 percent influence. This was a significant finding in that the response to dynamic loading due to traffic will be highly dependent on the quality of the subgrade soil. Rutting of up to 4.9 in. deep was observed in some locations. Those locations had California bearing ratio (CBR) readings of less than 2.

Only one AC pavement was tested, an AC thickness of 14 in. and the base course thickness was 12 in. *[13]*. The modulus of the AC and subgrade obtained from the FWD were approximately 1.35 times higher in the non-flooded area as compared to the flooded area 6 months after the flooding event. FWD readings taken 9 months after the flooding event showed similar modulus values between the flooded and non-flooded areas. The CBR values in the subgrade were around 10 times higher in the non-flooded areas relative the flood area. No structural failures were noted on the pavement, but erosion of the granular shoulder in regions near the high water line was observed.

As with the AC pavement, only one PCC pavement was tested, with a PCC pavement thickness of 9.8 in. and a 6 in. thick base course *[13]*. This section of roadway was subjected to rapid water currents which eroded some of the base course and embankment beneath the pavement. The voids were filled with flowable cement grout. Longitudinal cracks were observed in some panels where the base course had been removed due to erosion. Load transfer efficiency (LTE) ranged from 93 to 95 percent during testing. The k_{static} values varied from 55 to 73 psi which rated poor *[14]*. The CBR values were 20 on average in the top 12 in. of the subgrade.

Sultana et. al. conducted a study to evaluate the effects of flooding from an extreme weather event (January 2011) that occurred in South East Queensland *[15]*. The study was initiated by Austroads in 2013. Between the periods of 1967 to 2005, the direct damage due to floods was approximately $377 million Australian dollars per year. The total damage to the public infrastructure was estimated to range from $5 to $6 billion Australian dollars. Data was collected using an FWD on flooded and non-flooded roads. The data was used to calculate the layer moduli and CBR value for the subgrade. With that data, the modified structural number was calculated using equation (1) *[16]*.

$$SNC_i = 3.2 \times D_0^{-0.63} \quad (1)$$

where,
SNC_i = modified structural number at age ‘i’
D_0 = maximum deflection (mm) at load center at age ‘i’

Network level structural deterioration models for AC pavements [equation (2)] and sealed unbound granular pavements [equation (3)] were also used in their comparisons of flooded to non-flooded pavements *[17]*.

$$SNC_{ratio} = 0.991*(2 – EXP\ (0.00132\ x\ TMI_i + 0.256*(AGE_i / DL)) \quad (2)$$

$$SNC_{ratio} = 0.9035*(2 – EXP\ (0.0023\ x\ TMI_i + 0.1849*(AGE_i / DL)) \quad (3)$$

where,
SNC_{ratio} = current strength of pavement/subgrade relative to its initial strength (=SNC_i / SNC_0).
SNC_i = modified structural number at the time 'i' of measurement.
SNC_0 = modified structural number at the time 'i' of pavement construction.
TMI_i = Thornthwaite Moisture Index at the time 'i' of measurement.
AGE_i = age of pavement (number of years since construction or last rehabilitation).
DL = pavement design life (years)

After conducting a detailed statistical analysis comparing flooded roads to non-flooded roads, Sultana et. al. concluded that flooding caused up to a 50 percent decrease in structural number and that the subgrade CBR was reduced up to 67 percent as well.

Alam and Zakaria published a paper discussing the detrimental impact of perennial floods on the infrastructure of Bangladesh *[18]*. They noted two primary categories of damage to roadways: embankment slope failures and pavement failures. They conducted a parametric study using CBR tests from subgrade soil samples and Marshall stability and flow tests from AC pavement samples.

CBR tests were conducted on specimens at three compaction levels: 56 blows, 35 blows, and 10 blows. The specimens from the three compactive levels were submerged in water for 4, 7, 30, and 45 days. The four-day soak period was used as the control due to the fact that CBR values are normally determined after soaking the samples in water for four days. The reduction in CBR values (relative to the control) were 16.7, 29.6, and 37.5 percent for the 7, 30, and 45 day soak specimens, respectively.

AC specimens were prepared in the laboratory with an asphalt content of 4.75 percent. Four sets of samples were prepared and submerged in water for 4, 7, and 30 days with alternating drying and wetting cycles. Marshall stability and flow tests were performed on the samples. Based upon the test results, the flow of the AC mixture increased by 35, 50, and 93 percent for the 4, 7, and 30 day submerged samples. Regarding the stability of the AC, it decreased by 13, 19, and 26 percent for the 4, 7, and 30 day specimens.

The results of this laboratory experiment demonstrates the adverse effects that occur to both the AC pavement and subgrade when they are submerged for extended periods of time.

Mallick et al. conducted a study where "systems dynamics" was used to create a software package that calculated the critical time ($T_{critical}$) for AC pavement and unbound base course required to reach failure due to inundation *[19-22]*. Water entry into the AC pavement and underlying base course was calculated by modifying the Green and Ampt water infiltration equation *[23]*. The equation originally was developed to estimate the infiltration of water into soil as presented in equation (4). Mallick et.al. modified the equation to take into account the time required for water to infiltrate the AC pavement as presented in equation (5) *[19]*.

$$t = ((\theta_s-\theta_i)/ k_{effective})*[L_f – (h_L – \Psi_f)*[\ln((h_L+L_f- \Psi_f)/(h_L- \Psi_f))] \quad (4)$$

where,
θ_s = volumetric moisture content at saturation.
θ_i = initial volumetric moisture content.
L_f = thickness of (AC+base course), m.
Ψ_f = suction, m.
h_L = depth of ponded water, m.
t = time to infiltrate, m/s.
$k_{effective}$ = permeability, m/s.

$$k_{effective} = (h_{AC} +h_{base}) / ((h_{AC}/k_{AC}) + (h_{base}/k_{base})) \quad (5)$$

where,
h_{AC} = thickness of AC, m.
h_{base} = thickness of unbound base course, m.
k_{AC} = permeability of AC, m/s.
k_{base} = permeability of base course, m/s.

The systems dynamic model also included equations to take into account base course erosion if the pavement was near a stream and the reduction in tensile strength of the AC pavement due to inundation as presented in equations (6) and (7) *[24-25]*.

$$V_c = 0.35*D_{50}^{0.45} \quad (6)$$

where,
V_c = critical flow velocity (m/s).
D_{50} = particle size medium diameter (mm).

$$RTS(t) = RTS(i) - RRTS*t \quad (7)$$

where,
RTS(t) = retained tensile strength at any time t, %
RTS(i) = initial tensile strength (at construction), %
RRTS = rate of change (deterioration) in retained tensile strength, % per unit of time (years)
t = time at which the retained tensile strength is determined, years.

The results of their simulations using the systems dynamic approach indicated that the model was sensitive to (1) length of inundation period, (2) distress condition of the AC pavement and base course at the time of inundation, (3) thickness of AC pavement and base course, and (4) permeability of AC pavement and base course. The authors pointed out that the model could be improved with further research. The model can be used as a risk analysis tool for flood prone pavements.

Khan et al. conducted a series of studies where road deterioration (RD) models were developed for the parameters of rutting and IRI for inundated roads in Queensland, Australia *[26-30]*. The latest generation of models included performance models based upon the probability (P_r) of flooding, period of flooding, and loss of subgrade resilient modulus (M_rL) due to flooding. Khan et.al. discovered in their analyses that the gradient changes of rutting produced similar results to that of IRI *[26]*. Because of that models for rutting were not provided. The two new gradients proposed were $\Delta IRI/P_r$ and $\Delta IRI/M_rL$.

Monte Carlo simulations were used to test the new gradients. Simulations included (1) varying probabilities of flooding, (2) proposed $\Delta IRI/P_r$, (3) proposed $\Delta IRI/M_rL$, and (4) consequences of flooding. The results indicated that the models provided useful knowledge on the consequences of flooding for various types of sections. PCC and robust AC pavements were discovered to be the most flood resilient, which was consistent with the published literature *[9-15]*. The simulations indicated that the pavements with the poorest performance had the highest risk of flood probabilities. The advantage of the developed Monte Carlo models for $\Delta IRI/P_r$ and $\Delta IRI/M_rL$ is that it allows agencies to assess their pavements prior to flooding events and take action to minimize the risks.

Sultana et al conducted a state of the art literature review seeking to discover publications on the effects of flooding on roadway infrastructures *[31]*. Based upon their discoveries as well as research they conducted for others, they developed two mechanistic-empirical-deterministic deterioration models to predict rutting and roughness of flooded pavements *[31-33]*. They postulated that more effective decisions can be made regarding pavement rehabilitation based upon their models.

The model developed for rutting is presented in equation (8). It is a function of the time lapse between data acquired after flooding and prior to flooding. This model had a pearson correlation coefficient r^2 of 0.67 and a sample size (n) of 436.

$$\Delta Rut_{post\text{-}flood} = k_{rut} \times [(0.083 \times t^{0.85}) + (0.109 \times Rut_{pre\text{-}flood}) - 0.746)] \qquad (8)$$

where,
$\Delta Rut_{post\text{-}flood}$ = difference in pre-flood and post-flood rutting (mm).
k_{rut} = local calibration for rutting (dimensionless)
t = time lapse in rutting in days after flood (t<172 days)
$Rut_{pre\text{-}flood}$ = preflood rutting (mm).

The roughness model is presented in equation (9). It is also a function of the time lapse between data acquired after flooding and prior to flooding. This model had a pearson correlation coefficient (r^2) of 0.319 and a sample size (n) of 436.

$$\Delta IRI_{post\text{-}flood} = k_{rg} \times [0.039 + (0.027 \times t^{0.5})] \qquad (9)$$

where,
$\Delta IRI_{post\text{-}flood}$ = difference in pre-flood and post-flood IRI (m/km).
k_{rg} = local calibration for IRI (dimensionless)
t = time lapse in roughness (IRI) in days after flood (t<172 days)

Shamsabadi et al. conducted a study to determine the effects of snow storms and flooding events on the performance of highway pavements *[34]*. They did so by extracting pavement data from the Long Term Pavement Performance (LTPP) program and climate data from the NOAA database. The datasets used were from four states and covered a period of 17 years. Equation (10) presents the flexible pavement model developed for areas affected by snow storms, freeze thaw events, and large precipitation events developed by Jackson et al. *[35]*.

$$Ln(\Delta IRI+1) = Age(4.5FI + 1.78CI + 1.09FTC + 2.4PRECIP +5.39log(ESAL) / SN \quad (10)$$

where,
ΔIRI = change in International roughness index (m/km).
Age = pavement age (years).
FI = freezing index (degree-days when air temperatures are below and above zero degrees Celsius).
CI = cooling index (temperature relation to the relative humidity and discomfort).
FTC – freeze-thaw cycle.
PRECIP = precipitation.
ESAL = equivalent single axle load.
SN = structural number.

Equation (10) was further refined by Shamsabadi et al. as presented in equation (11). The authors wrote that the deterioration model could result in more realistic assessments of future costs, maintenance planning, and rehabilitation activities.

$$\%\Delta IRI = 5.09 – 2.5NIRI + 1.7NDepth – 1.74NDuration + 0.706ESAL*NDuration \quad (11)$$

where,
%ΔIRI = Percentage increase in IRI due to the snow storm.
NIRI = Normalized IRI of the section before the snow storm.
NDepth = Normalized depth of the snow storm.
NDuration = Normalized duration of the snow storm.
ESAL = equivalent single axle load (derived from traffic).

Elshaer assessed the mechanical responses of pavements during and after flooding in part by using models developed for the Mechanistic Empirical Pavement Design Guide (MEPDG) *[36-37]*. Elshaer used layered elastic methods to conduct the analyses in his dissertation. The objectives were to (1) determine analysis methods to evaluate post-flood pavements; (2) determine the performance of flooded pavements; (3) to obtain significant parameters following a flooding event; (4) develop a state of the art method to incorporate subgrade soil moisture into the analysis; (5) enhance knowledge on the effect of subsurface water on the load carrying capacity of pavements; (6) determine the stress dependency and moisture sensitivity of unbound materials; (7) observe the effect of suction and the resilient behavior on unbound materials; and (8) provide procedures to determine the failure time of flooded pavements.

The major conclusions derived from the research were, (1) incorporating the effects of suction into the analysis influenced the performance predictions; (2) the load carrying capacity is greater in coarse grain soils than fine grain soils; (3) the depth of the water table is more significant upon pavement performance for fine grain soils than coarse grain soils; and (4) load distribution from the tires to the pavement structure differ significantly as the water table returns to its preflood depth. The contents of this study establishes a framework that requires further validation using a wider variety of soils types as well as field validation.

Soil Physics and Seasonal Volumetric Change

Pavement surface and embankment distresses due to seasonal moisture variation in the base course, subgrade, foreslope, ditches, and backslope are both a national and international issue existing since the first hard surfaced pavements were constructed *[38-41]*. Clay soils, which are prevalent in many regions of Louisiana, can be particularly vulnerable to changes in moisture content, shrinking during drying (desiccation) and swelling during wetting (absorption). In some instances, soils with high silt contents may also exhibit volume changes and desiccation cracking *[42,43]*. Volume changes and/or tension cracks can be accelerated or increased when trees are present. Trees extract water from the soil, which in turn increases the suction stresses in the soil as well as the magnitude of moisture content changes due to the seasonal wetting and drying the embankment soil and base course.

Pavement surface distresses resulting from seasonal soil moisture content variation can be attributed to four major factors as well as their interactions:

1. Transverse and longitudinal volumetric change differential (due to wetting and drying) in the embankment, base course, and adjacent natural ground.
2. Desiccation cracking.
3. Dynamic settlement due to soil densification caused by soil suction stresses.
4. Slope failures.

Volumetric changes in the subgrade and/or base course differ in the travel lane(s) in that the volume change at the center line of the pavement differs significantly from the volume change at the pavement edge. Near the pavement edge, movement may be significant enough to cause damage as presented in Figure 4. Such a volumetric differential can manifest either as single or multiple longitudinal crack(s) beginning approximately 1 to 3 ft. from the pavement edge due to pavement bending (heave and subsidence) as presented in

Figure 4 *[44-48]*. As a result of continual bending, alligator cracking patterns have been known to occur in the asphaltic (AC) surface as presented in Figure 5. The volume change also occurs longitudinally along the travel lane(s) which can lead to bumps and depressions in the pavement. This in turn contributes to decreased ride quality due to the changes in the roadway profile.

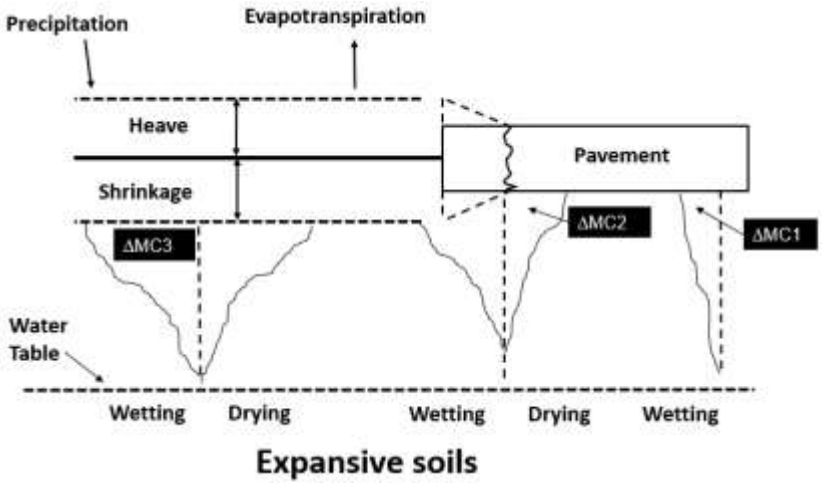

Figure 4
Effect of moisture change on pavement structure

Figure 5
Alligator cracking in AC surface

Longitudinal cracks in the pavement may also be caused by desiccation in the expansive clay subgrade. When the soil suction stresses induced by desiccation coupled with net normal stress exceed the tensile strength of the soil, a crack will form as shown in Figure 6 *[39-41]*. When this occurs beneath the pavement, it is possible for the crack to propagate through the pavement structure.

Figure 6
Parish road: St. Martin Parish

Slope failures may also occur due to seasonal moisture variation. If tension cracks develop in the embankment slope during desiccation, a failure plane may develop. Tension cracks create direct paths for water infiltration. This can quickly saturate the embankment reducing its shear strength which can lead to failure. Cracks as deep as 3 ft. and as wide as 2.5 in. have been measured by LTRC as presented in Figure 6. These cracks are probably due to a combination of distress mechanisms such as volumetric changes, desiccation cracking, and slope failures.

Damage Mechanisms Caused by Inundation

The pavement distress and soil physics phenomenon previously described were intended to illustrate what happens during normal seasonal wetting and drying events. Inundation of the roadway serves to exacerbate the swelling and shrinking of expansive soils by fully saturating (100 percent) the soil and base course.

For example, assume that that the volumetric moisture content (VMC) beneath the pavement (ΔMC1) normally ranges from 65 to 85 percent, and the VMC at the edge of the pavement (ΔMC2) normally ranges from 35 to 65 percent while the VMC at a location away from the pavement (ΔMC3) (natural ground) ranges from 15 to 55 percent seasonally; refer to Figure 4.

After an inundation event, it is possible and probable for the soil to fully saturate (VMC = 100 percent) at ΔMC1, ΔMC2, and ΔMC3. Once the flood waters recede and the roadway,

embankment, and natural ground become exposed to the atmosphere and sunlight, evaporation will occur. If it is in the spring and summer, evaporation will be even greater where trees are present due the transpiration of the trees and other flora. So instead of ΔMC1, ΔMC2, and ΔMC3 ranging from their normal VMC maximums of 85 percent, 65 percent, and 55 percent, they now range respectively from 100 percent to 65 percent, 100 percent to 35 percent, and 100 percent to 15 percent. Such changes in the VMC in an expansive soil will increase the magnitude of its swell, thus, leading to a larger range of ground movement due to swell. Furthermore, as evaporation and transpiration remove water from the ground and beneath the pavement surface, shrinkage will occur leading to subsidence in the ground. However, under this circumstance, the range between swelling and shrinking is greater than the normal range experienced for this area under normal seasonal variation. Such a range in movement can damage the pavement leading to premature failures and cracking with subsequent service life reductions. Figure 7 presents the general relationship of void ratio (e) versus VMC for an expansive soil. Through formulas, the volume change and subsequent change in height or ground movement can be calculated. As the soil varies in its mineralogical composition, so will the relationship between void ratio and VMC *[41-43]*.

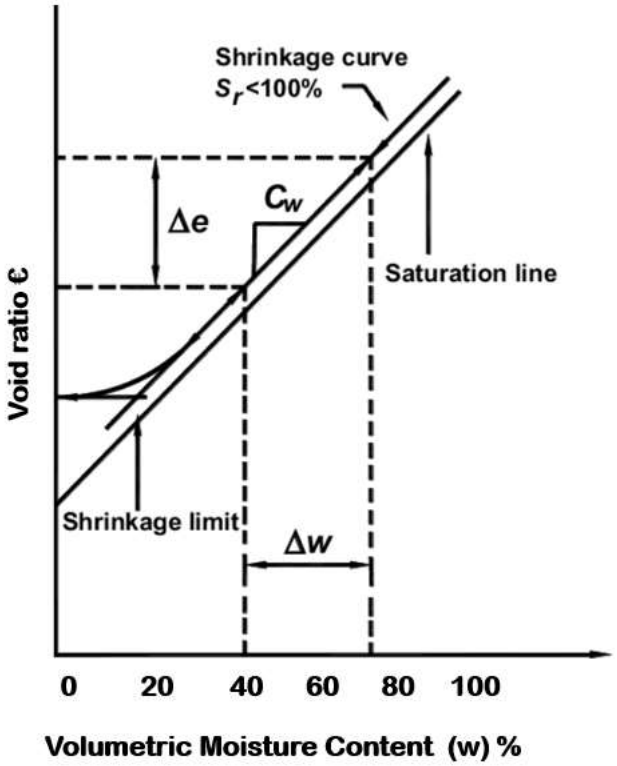

Figure 7
Volumetric moisture content versus void ratio

OBJECTIVE

The objective of this project was to conduct a structural assessment of inundated and non-inundated roads in Livingston Parish, Louisiana with the FWD. With FWD data, three parameters were calculated and statistically analyzed: SN_{eff}, D1, and subgrade M_r. The data from the three parameters were used to determine the effects of inundation on Livingston Parish's roadway system.

SCOPE

The scope of work for this project entailed conducting a structural assessment on the 400 miles of inundated roads in Livingston Parish's roadway system with the falling weight deflectometer and roadway cores to establish the thickness of the pavement layers. Ten percent of the 400 miles were sampled-tested and a similar amount of non-inundated roadways were sampled-tested in an attempt to have a balanced statistical analysis data set. Damage was established by converting the SN_{eff} into an equivalent amount of AC pavement.

METHODOLOGY

Experiment Design

As is the case with most inundation events, there were no pre-inundation structural testing data available for the roadway network in Livingston Parish *[9-36]*. Because of that, a "before and after" statistical comparison of the structural strength of the pavement system (pavement, base course, and subgrade) could not be performed. Instead, the statistical method of comparing treated to untreated roadway pavements with similar typical sections was employed. In this case, treated refers to roadways that were inundated during the August 2016, flood while untreated refers to the roadways that were not inundated.

Methods to Separate Inundated from Non-inundated Roadways

In a previous project, LTRC developed an approach to stratify inundated from non-inundated roadways, conduct statistical analyses on the results, and determine the associated costs with the measured damage *[9-12]*. These protocols were later modeled by others *[9-12]*. The Louisiana Governor's Office of Homeland Security and Emergency Preparedness (GOHSEP) asked LTRC to assemble said protocol's into a document for their review as presented in Appendix B.

LTRC began by determining the limits of roadway inundation in Livingston Parish. It should be noted that state or federal routes maintained by the Louisiana Department of Transportation and Development (DOTD) were not included in this study. LTRC began by obtaining a list of roadways from Livingston Parish with the perceived limits of inundation on those roadways. Next, LTRC searched the internet to attempt to locate flood maps for the August 2016 flood. Agencies such as National Oceanic Atmospheric Association (NOAA), United States Geographical Survey (USGS), National Aeronautics and Space Administration (NASA), and Federal Emergency Management Association (FEMA) were queried. LTRC discovered that FEMA had published a GIS-based map showing the boundaries of inundation along with a means of determining approximate depths of inundation *[49]*. Since this was an official publication from FEMA, it was used as the primary source of locating the inundation limits.

The mapping software used to assemble the roadway network and inundation limits was Google Earth version 7.3.2.5576 *[50]*. Google Earth contained the complete roadway network for Livingston Parish. The inundation map from FEMA for the August 2016 flood was imported into it. With the Google Earth features previously mentioned and the imported

FEMA map, LTRC began to search the roadway network for both inundated and non-inundated areas as presented in Figure 8. It proved to be a difficult task to locate non-inundated areas since it was estimated that at least 74 percent of Livingston Parish was inundated *[4-6]*. The colored areas on the map in Figure 8 represent areas that were inundated, while the areas with clearly visible satellite images were the non-inundated areas. The balloon shaped points in either green or yellow represent the beginning points of FWD testing locations. Yellow balloons represent the non-inundated (NF) areas and the number in front of it represents a unique identifier for each roadway in this study provided to LTRC by Livingston Parish officials, while the green balloons represent inundated (F) areas.

LTRC was unable to locate any sources where maps were available from the period of initial inundation to the period when all the flood waters had receded. Because of that, it was impossible to determine within a reasonable degree of certainty the various degrees of inundation periods for roadways in Livingston Parish so no attempt to statistically test for the effects of duration were conducted. Though depths of inundation could be determined from the FEMA data, LTRC did not test for the effects of depth of inundation because doing so was beyond the scope of work for this study.

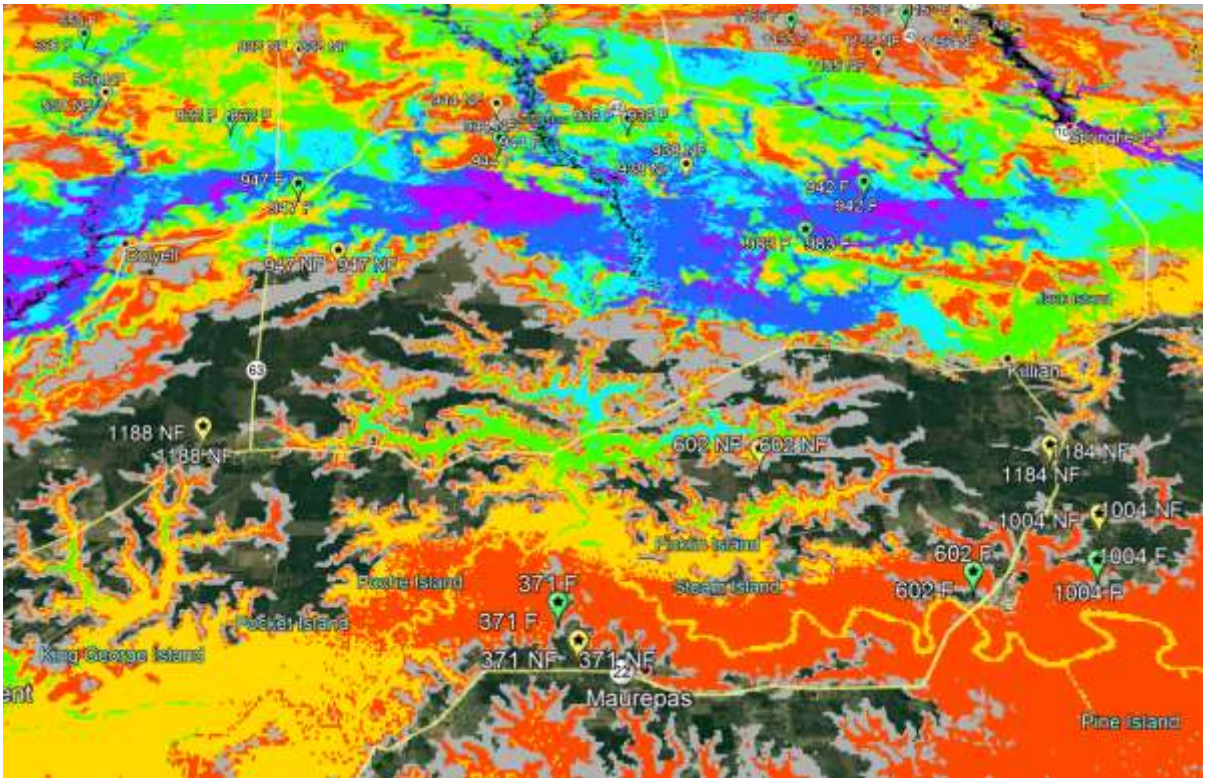

Figure 8
Maps showing inundated and non-inundated area in Livingston Parish, LA

Roadways Selected for Testing

Livingston Parish provided LTRC with a list of approximately 400 miles of roadways that were inundated. It was decided to conduct FWD testing on approximately 40 miles of those roadways. Livingston Parish does not have an established Pavement Management System (PMS) as does DOTD. Because of that, it had only a general idea of the thicknesses of the pavement and base course. In some instances, the type of base course was unknown. At the time of FWD testing (September 10 – 12, 2018), LTRC processed and analyzed the data using the pavement and base course thicknesses provided by Livingston Parish.

There were five groups used in the preliminary analysis (September 2018), all points, 4 in. thick, 3 in. thick, 2 in. thick, and 1.5 in. thick. Here "thick" refers to the thickness of the AC pavement provided by Livingston Parish. The preliminary results (September 2018) were based upon those assumptions. The results indicated that statistical differences between the inundated and non-inundated pavements existed only for the 3 in. thick and 2 in. thick groups. The methods and parameters used in that analysis were similar to those described in detail in the following sections of the methodology.

LTRC developed the approach where testing on the same roadway in the inundated and non-inundated areas was conducted when possible so as to minimize the chance of having a different pavement typical section and/or traffic loading. This minimized error in structural number determination due to factors such as different typical sections and/or roadway distresses due to varying traffic loading. Appendix A presents the roadways that were tested with the FWD and later cored to determine the actual pavement and base course thicknesses and type in May 2019.

Structural Testing

The structural number (SN) is an abstract number used to represent the overall structural strength of a pavement and its ability to sustain specified traffic loading for specified time periods *[14]*. The in-place structural number (SN_{eff}) is a measurement of existing roadways current overall structural strength and is commonly measured with the FWD *[14]*. In the design of pavements, DOTD considers 0.44 SN to be equivalent to 1 in. of AC pavement. Data from FWD testing may be used to determine the modulus value of each layer in the pavement system (pavement, base course, and subgrade) as well. For this study, three parameters were used to compare the inundated roadways with the non-inundated roadways described as follows.

1. **First Sensor Deflection (D1) (mils):** The deflection of the pavement at the load plate reflects the strength of the overall pavement structure. In general, for a given pavement system, higher deflections represent weaker pavement structures while lower deflections represent stronger pavement sections. Note: 1 mil = 0.001 in.
2. **Effective Structural Number (SN_{eff}) (dimensionless):** As mentioned previously, the effective structural number represents the effective structural strength of the existing pavement and base course, which, in this case was derived using formulas from the 1993 AASHTO design guide, deflections obtained from FWD testing, and pavement layer thickness determined by coring *[14]*. Of the parameters being analyzed, this one is the most valuable as it may be transformed into an equivalent thickness of AC pavement and therefore, can be monetized.
3. **Subgrade Resilient Modulus (M_r) (ksi):** The subgrade resilient modulus was determined using methods from the AASHTO 1993 design guide. It was then converted to its laboratory equivalent by multiplying it by 0.33 *[14]*.

Note: The thicknesses of the AC pavement and soil cement base course used in the computations of these three parameters were based upon coring and are outlined in Appendix A.

Statistical Analysis of Data

In this study, the Fisher ANOVA method was used to statistically compare inundated roadways with non-inundated roadways. The output from the statistical tests were assigned letters using the multiple comparison method *[51-52]*. Parameters that had similar letters inferred that they had statistically similar means and vice versa.

DISCUSSION OF RESULTS

Statistical Analysis

There were three sets of data subjected to ANOVA testing: all thickness group, 4 in. to 3 in. thick group, and 2.5 in. to 2 in. thick group. In this case, thicknesses are referring to the thickness of the AC pavement only as measured by coring. Regarding the all thickness group, its data were analyzed so as to determine if there were statistical differences between the inundated and non-inundated pavements as a whole. This can be considered a network analysis approach. Stratifying the data into 4 in. to 3 in. thick and 2.5 in. to 2 in. thick allowed LTRC to determine the amount of damage specifically for those thickness ranges. Due to the fact that very limited data was available for pavements whose AC thickness were either 1.5 in. or 1.0 in., a group was not constructed for this range. However, they were part of the all thicknesses statistical analyses group.

Statistical Analyses for All Thickness Groups

The analysis began by sorting the data into inundated and non-inundated groups for all points regardless of their thicknesses. The results of this testing regime are presented in Table 1. The ANOVA results indicated that there was a statistical difference for the parameter of SN_{eff} with the non-inundated (NF) group having the higher mean. This implies that the non-inundated group was stronger than the inundated group indicating that damage occurred due to inundation. The difference in the means (2.644 – 2.341) was 0.303 SN. As stated previously, 1 in. of AC is equivalent to 0.44 SN. Dividing 0.303 SN by 0.44 in. AC means that the damage was equivalent to 0.69 in. thick AC. It customary to round up to the nearest 0.5 in. which means the damage was equivalent to approximately 1.0 in. AC. The damage discovered here is within the range of damage caused by inundation reported by others *[9-12]*.

Table 1
Statistical analysis results for SN_{eff} for the all thickness group

Variable	N	Mean	Fisher grouping	
SN_{eff}_NF	231	2.644	A	
SN_{eff}_F	295	2.341		B

The results for the parameters of D1 and M_r are presented in Tables 2 and 3. Regarding the deflection at the first sensor (D1), the results indicated that a statistical difference existed between the inundated and non-inundated pavement. The mean value (D1) for the inundated data set (19.78) was higher than the non-inundated data set (16.15) indicating that it was 22.5

percent weaker. In the case of the subgrade M_r, the mean value (4.43) for the non-inundated group was higher than the mean value (3.972) for the inundated group. This implies that the subgrade beneath the inundated pavements were 10.3 percent weaker than the subgrade beneath the non-inundated pavements. Hence, all three parameters (SN_{eff}, D1, and M_r) indicated damage for inundated pavements. The damage discovered here is within the range of damage caused by inundation reported by others *[9-12]*.

Table 2
Statistical analysis results for D1 for the all thickness group

Variable	N	Mean (mils)	Fisher grouping	
D1_F	295	19.78	A	
D1_NF	231	16.15		B

Table 3
Statistical analysis results for subgrade M_r for all thickness groups

Variable	N	Mean (ksi)	Fisher grouping	
M_r_NF	231	4.43	A	
M_r_F	295	3.972		B

Statistical Analysis Results for 4 in. to 3 in. Thickness Group

The data set was sorted into pavements with AC thicknesses of 4 in. to 3 in. Having reduced the data set to this thickness range, they were sorted into inundated and non-inundated data sets and statistically analyzed using the Fisher ANOVA method. The results of the analysis for the SN_{eff} are presented in Table 4. The results indicated that the non-inundated group had a mean value (3.393), which was larger than the mean value (2.444) for the inundated group. This implies that damage occurred due to inundation. The damage (3.393 – 2.444) was 0.949 SN. This was converted to an equivalent thickness of AC (0.949 SN / 0.44 in. AC), which is 2.16 in. AC. Rounding up to the nearest 0.5 means that the damage was equivalent to 2.5 in. of AC for the 4 in. to 3 in. thickness group. The damage discovered here is within the range of damage caused by inundation reported by others *[9-12]*.

Table 4
Statistical analysis results for SN_{eff} for the 4 in. to 3 in. thickness group

Variable	N	Mean	Fisher grouping	
SN_{eff}_4 & 3 in_NF	55	3.393	A	
SN_{eff}_4 & 3 in_F	120	2.444		B

Tables 5 and 6 presents the results of the statistical analysis for the D1 and subgrade M_r parameters, respectively. The results for the D1 parameter indicated that the mean value

(19.23) for the inundated group was larger and statically different than the mean value (12.29) for the non-inundated group; hence the inundated pavement was a 56.5 percent weaker that the non-inundated pavement. Regarding the subgrade M_r, the statistical analysis indicated that the mean value (5.725) for the non-inundated group was larger and statistically different than the mean value (4.278) for the inundated group. This indicates that the subgrade M_r was 25.3 percent weaker in the inundated pavement as compared the non-inundated pavement. As discovered with the all thickness group, all three parameters (SN_{eff}, D1, and M_r) indicated damage due to the inundation event. The damage caused by inundation is within the range reported by others *[9-12]*.

Table 5
Statistical analysis for D1 for the 4 in. to 3 in. thickness group

Variable	N	Mean (mils)	Fisher grouping	
D1_4 & 3 in_F	120	19.23	A	
D1_4 & 3 in_NF	55	12.29		B

Table 6
Statistical analysis of the subgrade M_r for the 4 in. to 3 in. thickness group

Variable	N	Mean (ksi)	Fisher grouping	
M_r_4 & 3 in_NF	55	5.725	A	
M_r_4 & 3 in_F	120	4.278		B

Statistical Analysis Results for 2.0 in. to 2.5 in. Thickness Group

The data set was sorted into pavements with AC thicknesses ranging from 2 in. to 2.5 in. Having reduced the data set to this thickness range, they were sorted into inundated and non-inundated data sets and statistically analyzed using the Fisher ANOVA method. The results of the analysis for the SN_{eff} are presented in Table 7. The results indicated that the non-inundated group had a mean value (2.49) which was larger than the mean value (2.28) for the inundated group and that no statistical difference existed. Though no statistical difference existed, there was a difference of 0.21 SN between the inundated and non-inundated pavement. This is equivalent to approximately 0.5-in. thick AC using calculations shown previously. The difference in structural strength discovered here is within the range reported by others *[9-12]*.

Table 7
Statistical results for the SN_{eff} for the 2 in. to 2.5 in. thickness group

Variable	N	Mean	Fisher grouping
SN_{eff}_2 & 2.5 in_NF	132	2.49	A
SN_{eff}_2 & 2.5 in_F	153	2.28	A

Tables 8 and 9 present the results of the statistical analysis for the D1 and subgrade M_r parameters, respectively. The results for the D1 parameter indicated that the mean value (20.16) for the inundated group was larger and statically similar than the mean value (16.45) for the non-inundated group. Regarding the subgrade M_r, the statistical analysis indicated that the mean value (3.932) for the non-inundated group was larger and statistically similar than the mean value (3.751) for the inundated group. Hence the reduction in overall pavement stiffness (D1) and subgrade M_r were 22.6 percent and 4.6 percent, respectively. This damage is within the range reported by others *[9-12]*.

Table 8
Statistical analysis results for D1 for the 2 in. to 2.5 in. thickness group

Variable	N	Mean (mils)	Fisher grouping
D1_2 & 2.5 in_F	153	20.16	A
D1_2 & 2.5 in_NF	132	16.45	A

Table 9
Statistical analysis results for subgrade M_r for the 2 in. to 2.5 in. thickness group

Variable	N	Mean (ksi)	Fisher grouping
M_r_2 & 2.5 in_NF	132	3.932	A
M_r_2 & 2.5 in_F	153	3.751	A

CONCLUSIONS

Researchers discovered strong evidence of damage caused by inundation. Evidence supporting this claim was based on a structural assessment of inundated and non-inundated roadways in Livingston Parish, Louisiana, with the FWD. The statistical method of comparing treated (inundated) to non-treated (non-inundated) roadway pavements with similar typical sections were employed. Three structural parameters were examined SN_{eff}, D1, and subgrade M_r.

The data were sorted into three groups based on the thickness of the AC pavement: All data points (all thickness groups), 4 in. to 3 in. group, and 2 in. to 2.5 in. group. The statistical analysis of the entire set of data indicated that statistical differences existed for all three parameters, SN_{eff}, D1, and subgrade M_r. Regarding SN_{eff}, the difference between the mean values of the non-inundated and inundated roadways was 0.303 SN. This was converted to its equivalent thickness of AC pavement, which was approximately 1.0 in. The differences in the mean values for D1 indicated that the inundated pavements were approximately 22.5 percent weaker than the non-inundated pavements in terms of overall stiffness. The subgrade M_r was 10.3 percent weaker on the inundated pavements when compared to the non-inundated pavements.

Statistical comparisons on the 4 in. to 3 in. thickness group indicated that statistical differences existed for all three parameters, SN_{eff}, D1, and subgrade M_r as with the all thickness group. In the case, the differences in SN_{eff} was 0.949, which is equivalent to approximately 2.5 in. of AC. Regarding the D1 values, the results indicated that the inundated pavements were approximately 56.5 percent weaker than the non-inundated pavements in terms of overall stiffness. The subgrade M_r was approximately 25.3 percent weaker on the inundated pavements as compared to the non-inundated pavements.

Statistical differences in the three parameters, SN_{eff}, D1, and subgrade M_r for the 2.0 to 2.5 in. thickness group were not discovered; however, differences in magnitudes of the means for each parameter were discovered, all indicating that the inundated pavements were weaker than the non-inundated pavements. Regarding the SN_{eff}, the difference in means between the non-inundated and inundated pavements were 0.21 SN which is equivalent to approximately 0.5 in. of AC. The difference in stiffness between the inundated and non-inundated pavements based on the D1 parameter was approximately 22.6 percent, while the strength difference in subgrade M_r was approximately 4.6 percent.

REFERENCES

1. NOAA National Centers for Environmental Information (NCEI) U.S. Billion Dollar Weather and Climate Disasters (2018). https://www.ncdc.noaa.gov/billions/
2. Smith, A. and Matthews, J. "Quantifying Uncertainty and Variable Sensitivity within the U. S. Billion-dollar Weather and Climate Disaster Cost Estimates," Natural Hazards. 2015. DOI:10.1007/s11069-015-1678-x
3. Federal Emergency Management Administration, Significant Flood Events, 2018, https://www.fema.gov/significant-flood-events. Accessed September 17, 2018.
4. The Adovcate. http://www.theadvocate.com/louisiana_flood_2016/article_62b54a48-662a-11e6-aade-afd357ccc11f.html, Accessed. May 1, 2019.
5. Broach, D. The Times-Picayune. https://www.nola.com/weather/2016/08/how_many_people_houses_were_fl.html, Accessed. May 1, 2019.
6. Terrell, D. The Economic Impact of the August 2016 Floods on the State of Louisiana, Louisiana Economic Development, 2016.
7. Kopp, R. E., Horton, R., Little, C., Mitrovica, Oppenheimer, M., Rasmussen, D., Strauss, B. and Tebaldi., C. "Probabilistic 21st and 22nd century sea-level projections at a global network of tide-gauge sites," Earth's Future, 2, pp. 383–406, 2014. DOI:10.1002/2014EF000239
8. Buchanan, M., Oppenheimer, M., and Koop, R. "Amplification of Flood Frequencies with Local Sea Level Rise and Emerging Flood Regimes," IOP Publishing, Environmental Research Letters, 12 06-4009, 2017. https://doi.org/10.1088/1748-9326aa6cb3. Accessed September 17, 2018.
9. Gaspard, K., Zhang, Z., Gautreau, G., and Abufarsakh, M. "Impact of Inundation on Roadway Pavements: Case Study – LA 493" Louisiana Transportation Research Center, FHWA/LA.18/608, 2019.
10. Gaspard, K., Martinez, M., Zhang, Z., and Wu, Z. "Impact of Hurricane Katrina on Roadways in the New Orleans Area," Louisiana Transportation Research Center, Technical Assistance Report No. 07-2TA, 2006.
11. Zhang, Z., Wu, Z., Martinez, M., and Gaspard, K. "Pavement Structures Damage Caused by Hurricane Katrina Flooding," *Journal of Geotechnical and Geoenvironmental Engineering*, 135(5), pp. 633-643, 2008.
12. Helali, K., Robson, M., Nicholson, R., and Bekheet, W. "Importance of a Pavement Management System in Assessing Pavement Damage from Natural Disasters: A Case Study to Assess the Damage from Hurricanes Katrina and Rita in Jefferson Parish,

Louisiana.," In Proceedings of the 7th International Conference on Managing Pavement Assets, 10-21, 2008.
13. Vennapusa, P., White, D., and Miller, K. "Western Iowa Missouri River Flooding - Geo-Infrastructure Damage Assessment, Repair and Mitigation Strategies," Center f or Earthworks Engineering Research, Iowa State University, IHRB TR-638, 2013.
14. American Association of State Highway and Transportation Officials, "AASHTO Guide For Design of Pavement Structures," 1993.
15. Sultana, M., Chai, G., Martin, T., and Chowdhury, S. "A Study on the Flood Affected Flexible Pavements in Australia," In Proceedings of the 9th International Conference on Road and Airfield Pavement Technology, 2015.
16. Paterson, W., "Road Deterioration and Maintenance Effects: Models for Planning and Management," John Hopkins University Press, 1987.
17. Austroads, "Predicting Structural Deterioration of Pavements at a Network Level - Interim Models," Sydney, New South Wales, Australia, 2010.
18. Alam, M. and Zakaria, M. Design and Construction of Roads in Flood Affected Areas, Engineering Concern of Floods, ISBN 984-823-002-5, 2002.
19. Mallick, R., Tao, M., Daniel, J., Jacobs, J., and Veeraragavan, A. "Development of a Methodology and a Tool for the Assessment of Vulnerability of Roadways to Flood-Induced Damage," *Journal of Flood Risk Management* 10, pp. 301-313, 2017.
20. Forrester, J. World Dynamics, Cambridge MA: Wright-Allen Press, 1971.
21. Radzicki, J. "A Systems Dynamics Approach to Sustainable Cities," In the Proceedings of the 13th International Systems Dynamics Conference, 191-210, 1995.
22. Sterman, J. "Sustaining Sustainability: Creating a Systems Science in a Fragmented Academy and Polarized World," In M.P. Weinstein & R.E. Turner, eds. Sustainability Science: The Emerging Paradigm and the Urban Environment. Springer, pp. 21-58, 2012.
23. Green, W. and Ampt, G., "Studies of Soil Physics, Part I - The Flow of Air and Water Through Soils.," *Journal of Agricultural Science*, 4, 1-24, 1911
24. Briaud, J., "Case Histories in Soil and Rock Erosion: Woodrow Wilson Bridge," In the 9th Ralph B. Peck lecture. *Journal of Geotechnical and Geoenvironmental* Engineering, 134, (10) pp.1425-1447, 2008.
25. National Cooperative Highway Research Program , "Guide for Mechanistic-Empirical Design: Design Inputs," Transportation Research Board, 2004.
26. Khan, M., Mesbah, M., Ferreira, L., and Williams, D. "Estimating Pavement's Flood Resilience," American Society of Civil Engineers, *Journal of Transportation Engineering*, Part B: Pavements, 2017.
27. Khan, M. "Improvement of a Pavment Management System Incorporating Flooding,"

Ph.D Thesis, School of Civil Engineering, University of Queensland, St. Lucia, Australia. 2017.

28. Khan, M., Mesbah, M., Ferreira, L., and Williams, D "Development a Road Deterioration Model Incorporation Flooding," In the Proceedings of Transportation Institute of Civil Engineering, 167(5), pp. 322-333. 2014.
29. Khan, M., Mesbah, M., Ferreira, L., and Williams, D. "Development of Road Deterioration Models Incorporating Flooding for Optimum Maintenance and Rehabilitation Strategies," Road Transportation Research Journal Australia-New Zealand Research Practices, 23(1), pp. 3-24, 2014.
30. Khan, M., Mesbah, M., Ferreira, L., and Williams, D. "Assessment of Flood Risks to Performance of Highway Pavements, Proceedings," Institute of Civil Engineers-Transport, Thomas Telford, London. 2017.
31. Sultana, M., Chai, G., Chowdhury, S., Martin, Tim, Anissimov, Y., and Rahman, A. "Rutting and Roughness of Flood-Affected Pavements: Literature Review and Deterioration Models," American Society of Civil Engineers, *Journal of Infrastructure Systems*, 24(2): 04018006, 2018.
32. Sultana, M., Chai, G., Martin, Tim, and Chowdhury, S. Modelling the Postflood Short Term Behavior of Flexible Pavements, *Journal of Transportation Engineering*, DOI: 10.1061/(ASCE)TE,1943-5436.0000873, 04016042. 2016.
33. Sultana, M., Chai, G., Martin, Tim, and Chowdhury, S. "Modelling Rapid Deterioration of Flooded Pavements," Road Transportation Research, 25(2), 2016.
34. Shamsabadi, S., Tari, Y., Birken, R., Wang, M. "Deterioration Forecasting in Flexible Pavements Due to Floods and Snow Storms," In the Proceedings of the 7th European Workshop on Structural Health Monitoring, 2014.
35. Jackson, N., and Puccinelli, J. "Effects of Multiple Freeze Cycles and Deep Frost Penetration," Long-Term Pavement Performance Data Analysis Support: National Pool fund Study TPF-5(013), 2006.
36. Elshaler, M. "Assessing the Mechanical Response of Pavements During and After Flooding," Doctoral Dissertations 160. https//scholars.unh.edu/dissertation/160. 2017.
37. National Cooperative Highway Research Program, "Laboratory Determination of Resilient Modulus for Flexible Pavement Design," NCHRP Digest 285, Transportation Research Board, 2004.
38. Nelson, J. and Miller, D. Expansive Soils, Problems and Practice in Foundation, and Pavement Engineering. John E Wiley and Sons, 1992.
39. American Society of Civil Engineers, "Expansive Clay Soils and Vegetative Influence on Shallow Foundations," Geotechnical Special Publication Number 115,

2001.
40. Department of the Army USA, "Technical Manual TM 5-818-7, Foundations in Expansive Soils," September 1983.
41. Terzaghi, K., Peck, R., and Mesri, G. Soil Mechanics in Engineering Practice. John Wiley and Sons, 1996.
42. Fredlund, D. and Rahardjo, H. Soil Mechanics for Unsaturated Soil. John Wiley and Sons, 1993.
43. Lu, N. and Likos, W. Unsaturated Soil Mechanics. John Wiley and Sons, 2004.
44. Wise, J. and Hudson, W. "An Examination of Expansive Clay Problems in Texas" Center for Highway Research, The University of Texas at Austin, Research Report Number 118-5, 1971.
45. Sebasta, S. "Investigation of Maintenance Base Repairs Over Expansive Soils: Year 1 Report," Texas Transportation Institute, FHWA/TX-03/0-4395-1, 2002.
46. Zornberg, J., Prozzi, J., Gupta, R., Luo, R., McCartney, J., Ferreira, J., and C. Nogueira, C. "Validating Mechanisms in Geosynthetic Reinforced Pavements," Center for Transportation Research_The University of Texas at Austin, 2008
47. Steinberg, M., "Geomembranes and The Control of Expansive Soils in Construction," McGraw-Hill Professional, 1998.
48. Al-Rawas, A. and Goosen, M. "Expansive Soils-Recent Advances in Characterization and Treatment" Taylor and Francis, 2006.
49. FEMA, Flood maps for Livingston Parish, http://fema.maps.arcgis.com/apps/MapJournal/index.html?appid=44a483119d604255972ea7088ea852f0, Accessed August 30, 2018.
50. Google Earth, https://www.google.com/earth/, Accessed May 10, 2019
51. Neter, J. Kutner, M., Nachtsheim, C. and Wasserman, W. Applied Linear Statistical Models Irwin 3rd Edition, ISBN: 0-256-11736-5, 1996.
52. Day, R. and Quinn, G. "Comparisons of Treatments after an Analysis of Variance in Ecology," Ecological Monographs 59: pg 433-463. 1985.

APPENDIX A

Table 10
List of roadways tested in Livingston Parish (1 of 2)

Roadway No:	Roadway Name	Inundated condition	Test Interval	Test miles	AC thick.	Base course thick.	Base course type
550	S. Satsuma Rd.	Inundated	500'	0.95	3"	9"	S.C.
550	S. Satsuma Rd.	Non-Inundated	500'	0.95	3"	9"	(1)
947	Gum Swamp Rd.	Inundated	500'	0.95	2"	8"	S.C.
947	Gum Swamp Rd.	Non-Inundated	500'	0.95	2"	8"	S.C.
1188	Palmer Rd.	Non-Inundated	500'	0.95	2"	8"	S.C.
1183	Jack Allen Rd.	Inundated	300'	0.57	3"	8"	S.C.
1183	Jack Allen Rd.	Non-Inundated	300'	0.57	3"	12"	S.C.
147	Joe May Rd.	Inundated	300'	0.57	3"	9"	S.C.
147	Joe May Rd.	Non-Inundated	300'	0.57	3.5"	8"	S.C.
866	Brown Rd.	Inundated	500'	0.95	2"	12"	S.C.
866	Brown Rd.	Non-Inundated	500'	0.95	2"	13"	S.C.
155	Buddy Ellis Rd.	Non-Inundated	300'	0.57	2.5"	13"	S.C.
155	Buddy Ellis Rd.	Inundated	300'	0.57	3"	10"	S.C.
1187	Linder Rd.	Non-Inundated	500'	0.95	4"	12"	S.C.
341	Duff Rd.	Inundated	500'	0.95	3"	9"	S.C.
341	Duff Rd.	Non-Inundated	500'	0.95	3"	9"	(1)
186	Burgess Rd.	Inundated	300'	0.57	2"	6"	S.C.
186	Burgess Rd.	Non-Inundated	300'	0.57	4"	8"	S.C.
1186	Sims Rd.	Non-Inundated	500'	0.95	3"	7.5"	S.C.
434	Wildwood Dr.	Inundated	500'	0.95	2"	8"	S.C.
768	Charles Holden Rd.	Inundated	500'	0.95	2"	9"	S.C.
792	Red Oak Rd.	Non-Inundated	500'	0.95	2"	11"	S.C.
792	Red Oak Rd.	Inundated	500'	0.95	2"	6"	S.C.
944	Lobell Rd.	Non-Inundated	200'	0.38	2"	8"	S.C.
944	Lobell Rd.	Inundated	200'	0.38	3"	4"	S.C.

Note: (1) base tested negative for cement and was not used in study.

Table 11
Roadways tested in Livingston Parish (2 of 2)

Roadway No:	Roadway Name	Inundated condition	Test Interval	Test miles	AC thick.	Base course thick.	Base course type
938	Fire Tower Rd.	Inundated	500'	0.95	2"	14"	S.C.
983	Patterson Rd	Inundated	500'	0.95	2"	9"	S.C.
942	Hutchinson CC Rd	Inundated	500'	0.95	4"	13"	S.C.
1155	George White Rd.	Inundated	500'	0.95	2"	10"	S.C.
1155	George White Rd.	Non-Inundated	500'	0.95	2"	9"	S.C.
1152	W. Bates Rd.	Inundated	500'	0.95	2"	6"	S.C.
1152	Hungarian Presbyterian Chruch Rd.	Non-Inundated	300'	0.57	1"	8"	S.C.
1025	George Mashon Rd.	Non-Inundated	500'	0.95	1"	10"	S.C.
1025	George Mashon Rd.	Inundated	500'	0.95	3"	8"	(1)
1074	Ambrose Hoover Rd.	Inundated	500'	0.95	1.5"	8"	S.C.
1074	Ambrose Hoover Rd.	Non-Inundated	300'	0.57	2"	8"	S.C.
1056	Pea Ridge Rd.	Inundated	500'	0.95	2"	8"	S.C.
1069	Hutchinson Cemetary Rd.	Inundated	500'	0.95	2"	6"	S.C.
1056	Pea Ridge Rd.	Non-Inundated	500'	0.95	2"	8"	S.C.
1185	Henry White Rd.	Non-Inundated	500'	0.95	3"	10"	(1)
1184	Golden St.	Non-Inundated	500'	0.95	2"	12"	S.C.
371	Gunboat Landing Rd.	Non-Inundated	200'	0.38	2"	8"	(1)
371	Gunboat Landing Rd.	Inundated	200'	0.38	1.5"	9"	S.C.
629	Black Lake Club Rd.	Inundated	300'	0.57	4"	9"	S.C.
1004	Carthage Bluff Rd.	Non-Inundated	200'	0.38	2"	6"	S.C.
602	Bull Run Rd.	Inundated	300'	0.57	3"	10"	S.C.
602	Bull Run Rd.	Non-Inundated	300'	0.57	3"	8"	S.C.

Note: (1) base tested negative for cement and was not used in study.

APPENDIX B

Inundated Road Assessment Proposed Protocol

Based on the findings identified in the study, the Governor's Office of Homeland Security and Emergency Preparedness (GOHSEP) proposes that the following protocol be used to equate a monetary damage assessment for roadways inundated by floodwaters *[10]*:

1. Inundated and Non-Inundated Roadways
    a. Determine extents of submerged roadways, including inundation duration and depth.
        i. Use road maps (DOTD, parishes, cities, other); contour maps (USGS, other); flood maps (NOAA, USGS, FEMA, other); river levels (USGS, other); flood limits (DOTD staff, city, parish, FEMA, other); relevant photos (various sources); debris haul routes and landfills (DOTD staff, DEQ, DNR, other).
2. Obtain data from non-inundated control group by assuming that no pre-disaster local testing data is available, or utilize the pre-existing data if available, reliable and not out dated.
    a. Determine need to test entire inundated road network and selected control non-inundated control group or develop sample size based on parameters that mimic entire network (pavement type, subbase type, roadway type, age, etc.) with high degree of statistical confidence (i.e., 95%).
    b. Must have accurate knowledge of the roadway pavement type and thickness as well as base type and thickness
    c. Must have accurate knowledge of pavement type (asphalt, PCC, and composite).
    d. Knowledge of subgrade soil type may be beneficial (roadway coring and NCHRP)
3. If agency does not have accurate knowledge of any of the above, use a ground penetrating radar (GPR) with pavement coring at least every mile to establish the pavement and base course types and thickness.
4. Once all sources have been tabulated, upload into a geo-referenced software package such as ARCGIS, so that the information may be displayed visually and sorted based upon desired parameters.
5. Perform Structural Pavement Assessment for non-inundated control roadways and inundated roadways. Obtain test parameters for deflections from the first sensor (D1), effective structural number (SN_{eff}), and subgrade resilient modulus (M_r).
    a. Collect data with either a Falling Weight Deflectometer (FWD) or Continuous Deflection Measurement Device (CDMD) such as a Rolling Wheel Deflectometer (RWD) or Traffic Speed Deflectometer (TSD).
    b. Agency may use either FWD or FWD-CDMD as tools for assessment.

        i. If the FWD alone is used, tests should be conducted every two-tenths of a mile in both directions on two lane roads. With four or more lanes, testing should be conducted in the outside lanes in both directions.
        ii. If the FWD-CDMD combination is selected, then the CDMD will be used to test all roadways and FWD will be conducted every one-half mile to verify CDMD testing. Roadway lane and direction testing would be similar to that outlined in the FWD testing alone section.
6. Analysis of Data
    a. Use roadways tested in non-inundated areas as the "control section" group, and the roadways tested in the inundated areas as the "treated" group.
    b. Compare the control group statistically to the treated group using an ANOVA analysis.
    c. Stratify the data based on pavement types (PCC, AC, COMP), pavement thickness, and inundated duration.
    d. Analyze the control group vs. the treated group for Structural Loss (SN) for each comparable parameter.
7. Establish Structural Loss (SN) and equate to equivalent pavement thickness to quantify.
    a. Illustrate soil strength loss curve and roadway structural loss curve based on testing and study findings.
    b. See the following two tables: Table 10 presents the statistical test comparing the flooded to non-flooded for the parameters of D1, SN_{eff}, and M_r for the thickness groups for AC pavement; Table 11 presents the statistical testing used to determine the differences in strength between thickness groups.

Table 12
ANOVA for AC pavements by thickness

	Thickness Group (1)	D1						
		inundated			non-inundated			p-value
		n	mean	std dev	n	mean	std dev	
AC	A							
	B							
	C							
	Thickness Group (1)	SN_{eff}						
		inundated			non-inundated			p-value
		n	mean	std dev	n	mean	std dev	
AC	A							
	B							
	C							
	Thickness Group (1)	M_r						
		inundated			non-inundated			p-value
		n	mean	std dev	n	mean	std dev	
AC	A							
	B							
	C							

Note: (1) Number of thickness groups will be based on available data.

Table 13
Means test for AC pavement thickness groups

Group	Thickness Range (1)	D1	SN_{eff}	M_r
1	A	---	---	---
2	B	---	---	---
3	C	---	---	---

Note: (1) Number of thickness groups will be based on available data.

8. Develop cost estimate for repairs based on structural loss conversion to equivalent pavement in thickness of asphalt.
    a. Develop estimate for proposed FEMA request based on structural loss equivalent to restore streets to pre-disaster structural strength (delta SN) for flooded segments versus non-flooded control segments.
    b. Use local pricing to determine reasonable per unit costs (DOTD or local government average bid tabulations).
    c. Create estimate based on total impacted streets converted to applicable measurement (i.e., area, length, volume, etc.).

Recommendations

The following recommendations are intended to "streamline" the above process by using similar or average data as a reference for future use, saving both time and money.

1. Consider using prior disaster road study findings with aggregate road structural loss in lieu of current testing.
    a. Avoid time consuming and costly testing and engineering costs.
    b. Summarize prior findings from studies in a table with supporting documentation for FEMA.
2. Alternatively explore other options including destructive testing and/or other testing techniques.
    a. Cross-reference other FEMA approved disaster methods such as steel frame building damage repair projects for non-visible damage eligibility and reason to avoid destructive testing methods.

This public document is published at a total cost of $250
42 copies of this public document were published in this first printing at a cost of $250. The total cost of all printings of this document including reprints is $250. This document was published by Louisiana Transportation Research Center to report and publish research findings as required in R.S. 48:105. This material was duplicated in accordance with standards for printing by state agencies established pursuant to R.S. 43:31. Printing of this material was purchased in accordance with the provisions of Title 43 of the Louisiana Revised Statutes.